Delivery of FGF10 by implantable porous gelatin microspheres for treatment of spinal cord injury

YUNTAO GU*, GUANGYU WEN*, HAI ZHAO, HAO QI, YI YANG and TIANQIONG HU

Department of Spinal Surgery, The Second Affiliated Hospital of Hainan Medical University, Haikou, Hainan 570311, P.R. China

Received June 20, 2022; Accepted April 25, 2023

DOI: 10.3892/mmr.2023.13024

Abstract. Porous gelatin microspheres (GMSs) were constructed to enhance the neuroprotective effects of fibroblast growth factor 10 (FGF10) against spinal cord injury (SCI). The GMSs were prepared using a water-in-oil emulsion, followed by cross-linking, washing and drying. The blank GMSs had a mean particle size of 35 μm, with a coarse and porous surface. FGF10 was encapsulated within bulk GMSs via diffusion. To evaluate the effects of the FGF10-GMSs, locomotion tests were performed as a measure of the functional recovery of rats. Hematoxylin and eosin and Nissl staining were used to quantify tissue injury, and Evans blue staining was used to evaluate blood-spinal cord barrier restoration. Western blotting and TUNEL assays were employed to assess apoptotic activity. Immunohistochemical staining of neurofilament antibodies (NF200) was used to evaluate axonal rehabilitation. Compared with the groups intravenously administered FGF10 alone, disruption of the blood-spinal cord barrier and tissue injury were attenuated in the FGF10-GMS group; this group also showed less neuronal apoptosis, as well as enhanced neuronal and axonal rehabilitation. Implantable porous GMSs could serve as carriers for FGF10 in the treatment of SCI.

Introduction

Spinal cord injury (SCI) can induce sudden memory loss, as well as loss of motor function on the distal side (1). Primary SCI reflects the direct mechanical impact of trauma on the spine, while secondary injury involves a complicated series of molecular processes, including local edema, ionic homeostasis disruption, focal bleeding, ischemia, inflammation and oxidative stress. Typically, apoptosis leads to progressive degeneration in cases of SCI (2,3). Decompression, medications and prevention of secondary complications are important for post-SCI functional recovery. Compounds aiding the recovery of neurological function post-SCI have been used to protect surviving tissues against degeneration; these substances promote axonal regeneration and suppress inflammation and glial scarring (4-7).

Fibroblast growth factor 10 (FGF10), also known as keratinocyte growth factor 2, is a basic protein consisting of 84-246 amino acids. It interacts mainly with embryonic epithelial cells, stromal cells, fibroblasts and organs including the liver, lung and intestine. FGF10 plays a role in the signaling of epithelial mesenchymal cells during embryonic development, promotes the formation and development of glands, and stimulates the development of internal organs (8,9). A neuroprotective effect of FGF10 has been demonstrated, and it can inhibit inflammation via the PI3K/Akt pathway to protect against acute brain injury (10). FGF10 promotes peripheral nerve regeneration by eliciting a PI3K/Akt signaling-mediated antioxidant response (11). Furthermore, FGF10 activates the FGFR2/PI3K/Akt signaling pathway and suppresses the activity of microglia/macrophages associated with TLR4/NF-κB-dependent neuroinflammation, thereby enhancing functional recovery after SCI (12).

FGFs and their receptors have a wide range of biological function via regulation of mitosis, survival, migration and differentiation (13). There are also evidences for the potential of FGF signaling on the progression of tumor (14). For most FGFs, malignant transformation is a potential risk (15). However, it has a wide range of clinical applications as a drug and exhibits favorable safety (16). There is little evidence that FGF10 can promote the malignant transformation of neurological tissue, and the spinal cord itself is not prone to canceration. Therefore, it is still considered that FGF10 delivery has huge potential when it was used in the hyperacute period in SCI.

However, FGF10 should not be administered systemically. First, as a macromolecular protein, systemic FGF10 may induce enzyme degradation, and it struggles to penetrate the blood-spinal cord barrier (BSCB). Second, FGF10 may induce mitosis, which can cause cancers within normal tissues. To overcome these drawbacks of protein-based medications, an *in situ* drug delivery system can be used to deliver therapeutics

Correspondence to: Dr Yi Yang or Dr Tianqiong Hu, Department of Spinal Surgery, The Second Affiliated Hospital of Hainan Medical University, 368 Yehai Avenue, Haikou, Hainan 570311, P.R. China
E-mail: yangyi201901@126.com
E-mail: hutianqiong2211@126.com

*Contributed equally

Key words: fibroblast growth factor 10, porous gelatin microspheres, spinal cord injury, blood spinal cord barrier, apoptosis

to the injured site. Due to its non-toxicity and biodegradability, gelatin is the preferred protective agent for depot preparations. In a previous study, locally implanted basic FGF (bFGF) and bone morphogenetic protein (BMP) were slowly released from a gelatin sponge, thus facilitating the regeneration of tracheal cartilage (17). Gelatin microspheres (GMSs) are widely used to deliver various growth factors, including BMP2, bFGF and vascular endothelial growth factor, as well as plasmids and stem cells, thereby facilitating the remodeling and regeneration of tissues (18-20). Compared with administration of free bFGF, bFGF/GMSs group results in a less necrosis, less infiltration of inflammatory cell, and a decreased the cavity ratio and less apoptotic cells in injured spinal cord, and exerts improved effect on motor function (20). The administration of human recombinant osteopontin/GMSs at 1 h post-ischemic brain reduced the mean infarct volume by 81.8% compared with that of the untreated control group and extended the therapeutic window at least to 12 h post-ischemic brain, demonstrating a markedly enhanced therapeutic potency of GMSs for the use of osteopontin in the post-ischemic brain (18). These studies suggested that GMS-mediated drug delivery has huge potential in the hyperacute period of neurological injury.

In the present study, porous GMSs were synthesized using a simple FGF10-encapsulating procedure. More specifically, GMSs loaded with FGF10 were administered to SCI rats; FGF10 was then slowly released at the site of injury. Behavioral tests were subsequently performed to assess the neuroprotective effects of FGF10-loaded GMS, which were also assessed by histopathology and apoptosis analyses.

Materials and methods

Reagents and antibodies. Every reagent utilized in the present study is commercially available. FGF10 was provided by Grost Biotechnology. Anti-caspase-3 (cat. no. 9661), anti-neurofilament (NF200, cat. no. 2836) and anti-β-actin primary antibodies (cat. no. 4967) and donkey anti-rabbit polyclonal IgG-HRP secondary antibody (cat. no. 7074) were obtained from Cell Signaling Technology, Inc.

GMS fabrication. First, GMSs were synthesized via water-in-oil (w/o) emulsion crosslinking, as previously described (17) with certain modifications. In brief, the 15% gelatin solution (w/v) was first synthesized, followed by dissolution of NaCl (0.2 g) in gelatin solution (4 ml; aqueous phase). Then, the aqueous phase was introduced dropwise into paraffin solution (40 ml) that contained 1.5% spann-80 and was heated to 50˚C. The mixture was subjected to a 30-min emulsification at 137 x g under paddle stirring. After cooling in an ice bath, the w/o emulsion was stirred for 30 min to spontaneously gelate the gelatin aqueous phase. Thereafter, a paraformaldehyde/isopropanol (40 ml, 5:35, v/v) solution was introduced into the w/o emulsion, NaOH was added to adjust the solution pH to 9.0, and the mixture was stirred for an additional 3 h for microsphere crosslinking. Subsequently, the samples were centrifuged at 1,000 x g to collect microspheres at room temperature. Residual oil was removed from the surface by washing repeatedly with isopropanol, followed by overnight drying under vacuum. Finally, NaCl (pore-forming agent) was removed by rinsing the microspheres thrice with distilled water, followed by further drying under vacuum. As a control, normal microspheres were prepared by the same process, except that NaCl was not added.

FGF10-loaded GMS preparation. FGF10-loaded GMSs were fabricated as previously described (20), with certain modifications. In brief, 0.3 mg/ml FGF10 aqueous solution was added to dry GMSs (100 mg) to encapsulate FGF10. The suspension was then maintained for 4 h under ambient conditions. Distilled water (300 μl) was used to rinse the FGF10/GMS mixture twice for removal of non-encapsulated FGF10. FGF10-loaded GMSs were then harvested for lyophilization, followed by annealing via a 12-h incubation using 10% human serum albumin (MilliporeSigma) at 37˚C. Immediately before injection, FGF10-loaded GMSs were dried by adding sterile phosphate-buffered saline (PBS; pH 7.4), and a 50-μl microsphere suspension was prepared for each animal. Meanwhile, sterile PBS was added to hydrate the unloaded dry microspheres used as a control.

Encapsulation efficiency. An enzyme-linked immunosorbent assay (ELISA) kit (cat. no. SEKH-0425; Beijing Solarbio Science & Technology Co., Ltd.) was used to determine the encapsulation efficiency. Briefly, 0.3 mg/ml FGF10 aqueous solution was introduced into the dry GMSs at various ratios (50, 100, 200, 300, or 500 μg FGF10/l00 mg dry GMSs); the suspension was then maintained for 4 h under ambient conditions. The FGF10/GMS mixture was rinsed twice with distilled water (300 μl) to remove non-encapsulated FGF10. After rinsing, the supernatant was harvested by centrifuging for 2 min at 800 x g at room temperature. An ELISA kit was then utilized to quantify the FGF10 level within the supernatant. The following formula was applied to determine the loading efficiency for the FGF10-loaded GMSs: Loading efficiency (%)=(FGF10 within supernatants)/total FGF10x100. Each sample was tested in triplicate.

Microsphere characterization. Fluorescein isothiocyanate-labeled FGF10 (FITC-FGF10) was used to prepare FITC-FGF10-loaded GMSs for *in vitro* release analysis, which was conducted using a previously described method (21) with slight modification. Specifically, FITC-FGF10-loaded GMSs (50 mg) were dispersed in PBS (1.5 ml) and then placed in a thermostatic oscillator. Microspheres were subjected to centrifugation for 5 min at 1,000 x g at pre-set times. After collecting the supernatant (150 μl), freshly prepared PBS was added to the system volume, such that the volume remained the same. A microplate reader (Thermo Fisher Scientific, Inc.) was used to quantify the fluorescence intensity of the samples at 495 and 525 nm. The fluorescence intensity of encapsulated FITC-FGF10 was considered analogous to that of the FITC-FGF10 solution, which was obtained by dissolving FITC-FGF10 in a volume identical to that of the release medium. This formula was utilized to determine the cumulative release rate of FITC-FGF10 from FITC-FGF10 microspheres *in vitro*.

Rat SCI model. Female Sprague-Dawley (SD) rats (n=48; age, 8-10 weeks) weighing 240-260 g were used in the experiments. The animals were raised in the laboratory under standard

conditions (20-24˚C, 50-55% humidity, 12-h light/dark cycle) with free access to food and water. Each rat was intraperitoneally injected with 50 mg/kg pentobarbital sodium for anesthesia. Thereafter, laminectomy was performed at the thoracic vertebra (T9-T10). After fully exposing the spinal cord, 30 g vascular clips (Oscar, China) were used to induce a moderate crushing injury for 1 min (22). The rats were randomized to the SCI (n=36) and sham groups (n=12); for rats in the sham group, an identical process was performed except that no crushing injury was induced. Lesions were subsequently injected with 20 μl FGF10 solution (n=12)/FGF10-loaded microspheres (60 μg/rat, n=12) using a 16-G needle. An equivalent amount of saline was injected into rats in the SCI (n=12) and sham groups. Postoperatively, all animals were returned to their original environment, with manual bladder expression performed twice per day until bladder function was restored. All animals were aseptically collected after euthanasia via CO_2 inhalation (40% vol/min for 5 min), and relevant spinal cords were removed for further experiments. The present study was approved by the Animal Care and Use Committee of Hainan Medical University (approval no. 2019-45; Haikou, China).

Recovery of locomotion. To assess recovery of locomotion post-SCI, the Basso, Beattie and Bresnahan (BBB) locomotor rating scale was used, together with a previously described incline plane test (23). Briefly, BBB scores reflect joint movement and muscle strength, where a score of 0 indicates complete paralysis and 21 normal locomotion. Two incline plane test positions (left or right side up) were used; instances where rats were able to maintain their position for 5 sec without falling were recorded.

Hematoxylin-eosin (H&E) and Nissl staining. To quantify necrotic tissue in the spinal cord cavity area postoperatively, all animals were sacrificed on day 28 to collect spinal cord tissues, which were subjected to paraffin embedding. Subsequently, 5-μm transverse slices were obtained and stained with H&E for 5 min at room temperature. The transverse sections were also treated with 1% cresyl violet acetate for 20 min at room temperature for Nissl staining to measure surviving neuronal cells.

Immunohistochemical staining. The primary antibody against NF200 (1/500) was used to incubate 5-μm transverse spinal cord sections overnight at 4˚C, followed by further incubation with the secondary antibody for 1 h at 37˚C. An optical microscope (ECLIPSE Ti-S; Nikon, Corporation) was used for image acquisition. Thereafter, technicians blinded to the treatments counted the positively stained cells in every mesencephalic section in the striatum. Image-Pro Plus software (version 7.0; Media Cybernetics, Inc.) was used to quantify cell density.

TUNEL apoptosis assay. The one-step TUNEL Apoptosis Assay Kit (Roche Diagnostics GmbH) was used to detect *in vivo* DNA fragmentation. To test apoptotic DNA fragmentation, animals were sacrificed and spinal cord tissues were collected, which were fixed in 4% polyformaldehyde for 24 h at room temperature and then subjected to paraffin embedding. Vertical slices (5 μm) were deparaffinized via propyl glycol for 30 min in room temperature and rehydrated via a gradient concentration of alcohol at room temperature, and were then incubated with 0.1% Triton X-100 for 15 min on ice. Apoptotic cells in the tissue sections were stained with TUNEL Apoptosis Assay Kit (Roche Diagnostics GmbH), according to the manufacturer's instructions. A total of 50 μl terminal deoxynucleotidyl transferase was mixed with 450 μl fluorescein-labeled deoxyuridine triphosphate. The slides were treated with the reaction mixture for 1 h at 37˚C and with DAPI (5 μg/ml) for 8 min at room temperature. Images in five fields were captured using the confocal ECLIPSE Ti-S microscope (Nikon Corporation; magnification, x40) to measure the apoptotic level.

Measurement of BSCB disruption. Evans blue (EB) dye was used to analyze BSCB disruption, as previously described by the authors (24). In brief, after SCI induction, each rat was injected with 2% EB dye (4 ml/kg) on day 1 via the tail vein. After 2 h, anesthesia was administered and sacrifice performed, and 30-μm coronal spinal cord slices were prepared. A confocal fluorescence microscope was used to observe EB fluorescence intensity.

Western blot assay. Spinal cord tissue from T8 to T11 was obtained at 7 days after operation. Briefly, tissue was lysed using radioimmunoprecipitation buffer (MilliporeSigma) containing protease and phosphatase inhibitors (1 mM). Following the addition of bicinchoninic acid reagent for determining protein concentration, equal amounts of proteins (50 μg) were subjected to 10% gel separation, followed by transfer onto a polyvinylidene difluoride membrane (Bio-Rad Laboratories Inc.). Thereafter, 5% (w/v) milk (Bio-Rad Laboratories, Inc.) was utilized to block the membrane for 90 min at room temperature, followed by incubation with the primary antibody (anti-cleaved-caspase-3) at 4˚C overnight and incubation with the secondary antibody for 60 min at room temperature. The ChemiDoc XRS$^+$ imaging system (version 5.2; Bio-Rad Laboratories, Inc.) was used to visualize the signal.

Statistical analysis. One-way ANOVA followed by Tukey's post hoc test was utilized to compare more than two groups using GraphPad Prism 5.0 (Dotmatics). $P<0.05$ was considered to indicate a statistically significant difference. Results are expressed as the mean ± SD.

Results

FGF10 encapsulation within porous microspheres. To determine the maximum FGF10 load, FGF10 at varying levels was mixed with freeze-dried microspheres (100 mg) and incubated for 12 h. The actual FGF10 encapsulated level within microspheres was then quantified (Fig. 1A) and increased according to the initial quantity used. When the added FGF10 increased, the encapsulated FGF10 also increased accordingly and after the addition of 200 μg FGF10, the encapsulated FGF10 reached the maximum (200 μg/100 mg). To investigate the distribution of encapsulated FGF10 within the microspheres, FITC-FGF10 was encapsulated in porous GMSs by an identical process. A uniform distribution of green fluorescence was observed

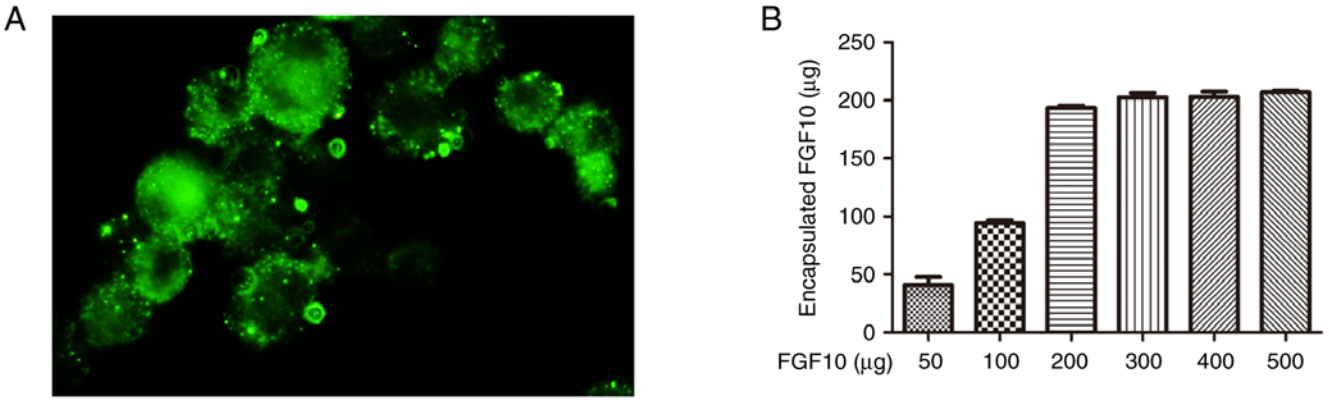

Figure 1. Encapsulation of FGF10 in porous microspheres. (A) Morphology of fluorescein isothiocyanate-labeled FGF10-loaded microspheres under fluorescence microscopy. (B) Correlation between the amount of FGF10 encapsulated in porous gelatin microspheres and the amount actually delivered. FGF10, fibroblast growth factor 10.

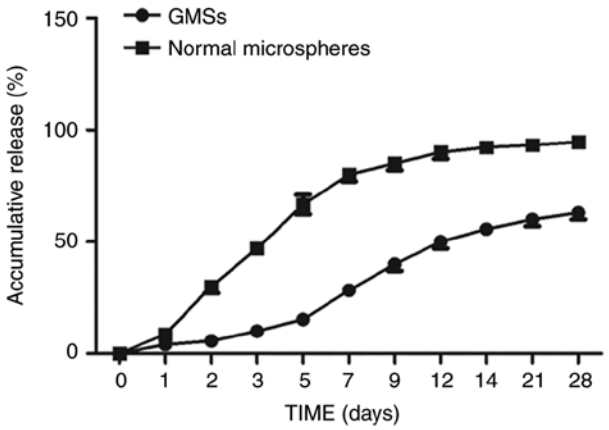

Figure 2. *In vitro* release of fibroblast growth factor 10 from porous microspheres and normal microspheres. GMSs, gelatin microspheres.

within bulk microspheres, reflecting high permeability of the intact microspheres to FGF10 (Fig. 1B).

Sustained release of FGF10 from FGF10-GMSs. To assess sustained release of FGF10 from GMSs, an *in vitro* release assay was used. The cumulative release of FGF10 from GMSs is demonstrated in Fig. 2. Normal GMSs rapidly released FGF10 in short bursts; ~30% of the encapsulated FGF10 was released within the initial 48 h, with complete release being achieved within 2 weeks. By contrast, porous microspheres continuously and gradually released FGF10 over 2 weeks, with no distinct burst release pattern observed within the first 48 h. On day 28, the proportion of encapsulated FGF10 released was only ~65%. The difference between normal microsphere and porous GMSs may be attributed to the distribution difference of FGF10 in the microsphere. Briefly, the burst FGF10 release of microsphere was dependent on the FGF10 absorbed on the surface of microsphere. Compared with dense and of little porosity surface of normal microsphere, the encapsulated FGF10 in porous GMSs homogenously distributed inside the bulk porous microspheres without a significant adsorption on their surfaces, making the diffusion pathway along which FGF10 released from microsphere longer.

FGF10-GMSs promote locomotor recovery after acute SCI in vivo. The BBB locomotor rating scale and incline plane test scores were used to assess the therapeutic effect of FGF10-GMSs. The sham group had normal BBB scores (21 points; Fig. 3). At 1 and 3 days after contusion, there was no significant difference in BBB scores among the FGF10-GMS, FGF10 and SCI groups. Compared with the SCI group, notable behavioral changes in the FGF10-GMS group were observed at 14 days ($P<0.05$). At 21 and 28 days, rats in the FGF10-GMS and FGF10 group exhibited favorable motor function recovery (Fig. 3A), particularly those in the FGF10-GMS group. The incline plane test results were consistent with the BBB locomotor rating scale scores (Fig. 3B); GMSs enhanced the functional improvement observed in SCI rats after FGF10 administration.

FGF10-GMSs improve histological injury in SCI rats. According to the H&E and Nissl staining results, destruction of central gray and peripheral white matter was most pronounced in the SCI group and was accompanied by obvious motor neuron loss in the anterior horn. Compared with the SCI and FGF10 groups, less necrosis, karyopyknosis and infiltrating polymorphonuclear leukocytes were observed in the FGF10-GMS group, along with a significantly smaller proportion of necrotic tissue in the spinal cavity (Fig. 4).

FGF10-GMSs attenuate BSCB disruption after SCI. The intensity of EB staining in spinal cord sections was markedly weaker in the FGF10 group compared with the SCI group as revealed in Fig. 5A, suggesting that FGF10 enhanced the integrity of the BSCB after SCI. However, the results indicated that the BSCB was best protected in the FGF10-GMS group. To quantify the leakage of high molecular weight molecules, FITC-dextran was injected into the tail vein. The intensity of the FITC-dextran signal was significantly lower in the FGF10 than SCI group (Fig. 5B and C).

FGF10-GMSs promote regeneration of injured neurons in SCI rats. NF proteins, including NF200, are markers of neuronal repair (25). Immunofluorescence staining was conducted to detect NF200 (Fig. 6). In the SCI group, NF200-positive fibers showed obvious degradation, along

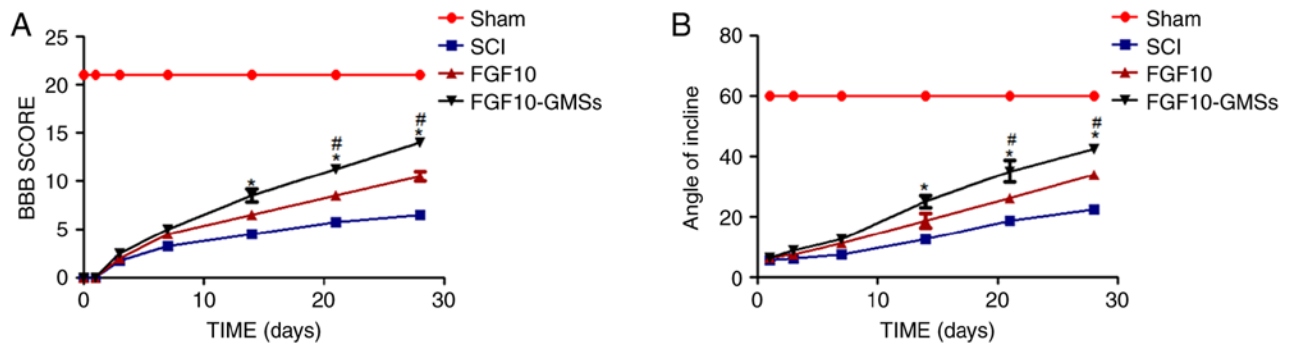

Figure 3. FGF10-GMSs enhance recovery of locomotor function following acute SCI *in vivo*. (A and B) BBB scores and results of the incline plane test were performed to measure the motor function recovery in each group. The data are presented as the mean ± SD. *P<0.05 vs. SCI groups and #P<0.05 vs. FGF10 groups. FGF10, fibroblast growth factor 10; GMSs, gelatin microspheres; SCI, spinal cord injury; BBB, Basso, Beattie and Bresnahan.

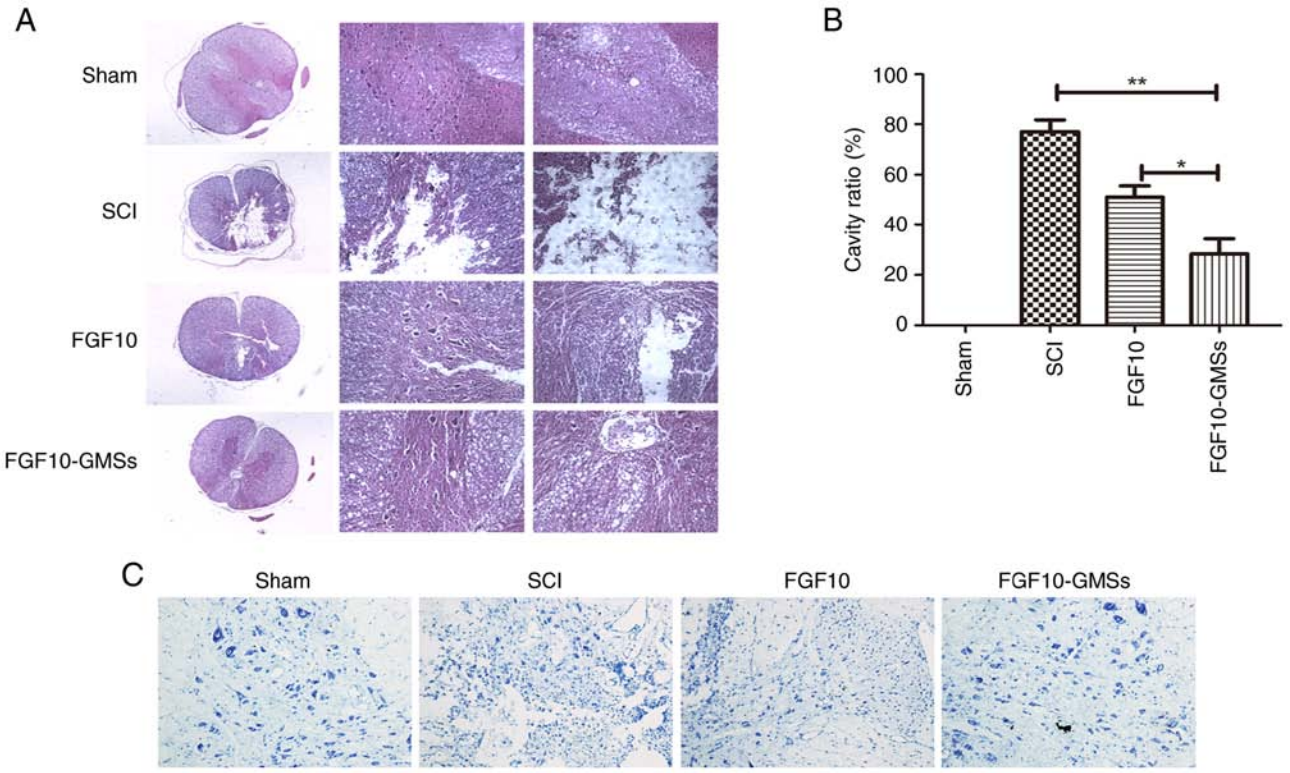

Figure 4. FGF10-GMSs improve histological injury in SCI rats. (A and B) Results of hematoxylin and eosin staining on postoperative day 28 and quantitative comparison of cavity necrotic tissue in the spinal cord cavity of each group at various time points (scale bar, 200 μm). (C) Nissl staining for surviving neurons on postoperative day 28 was performed to evaluate the apoptotic level of spinal tissue in each group. The data are presented as the mean ± SD. *P<0.05 and **P<0.01. FGF10, fibroblast growth factor 10; GMSs, gelatin microspheres; SCI, spinal cord injury.

with broken axons. While the FGF10 group exhibited an increase in NF200 expression around the lesion compared with the SCI group, this increase was even more marked in the FGF10-GMS group.

FGF10-GMSs inhibit apoptosis in SCI rats. Caspase-3 initiates apoptosis signaling (26). The results of western blotting of caspase-3 are presented in Fig. 7A and B. Caspase-3 expression in the SCI group was obviously enhanced 28 days after injury compared with uninjured rats. Apoptosis was suppressed to a greater extent in the FGF10-GMS group than in the FGF10 and SCI groups. TUNEL assay was also conducted to detect apoptosis and yielded similar results; the number of TUNEL-positive cells 28 days after FGF10-GMS treatment was significantly decreased compared with the FGF10 group (Fig. 7C).

Discussion

SCI may induce cystic cavity formation and neuronal loss, thereby inhibiting axonal regeneration. Although great progress has been made in the treatment of SCI, no optimal clinical strategy has been established, and relatively few therapeutics have been developed. Numerous factors limit the capacity for spontaneous spinal cord regeneration, including insufficient growth-promoting substances and the expression of growth

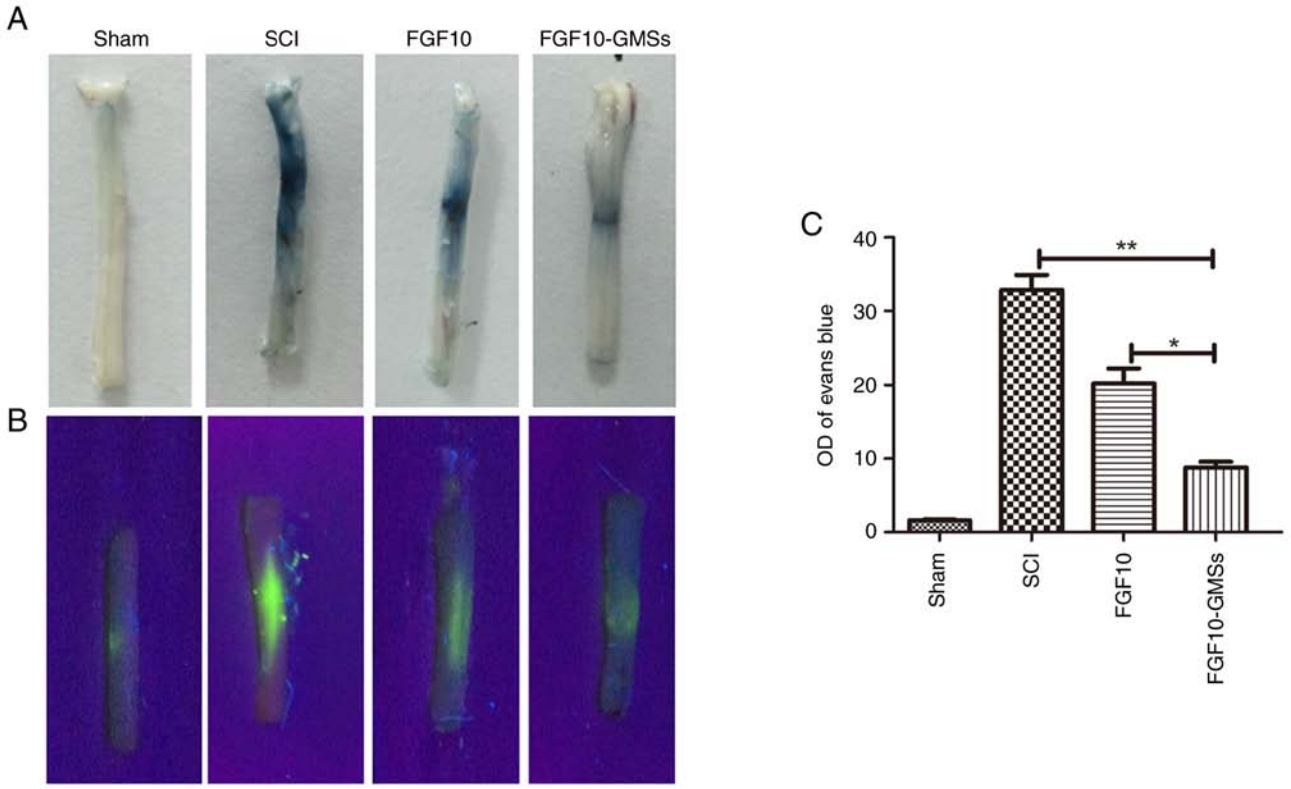

Figure 5. FGF10-GMSs attenuate BSCB disruption after SCI. (A) Representative images of Evans blue staining were performed to evaluated BSCB disruption of whole spinal cords on postoperative day 1. (B) Representative confocal images were further used to measure the BSCB disruption. (C) Quantitative comparison of fluorescein isothiocyanate-dextran staining intensity between each group. The data are presented as the mean ± SD. *P<0.05 and **P<0.01. FGF10, fibroblast growth factor 10; GMSs, gelatin microspheres; BSCB, blood-spinal cord barrier; SCI, spinal cord injury.

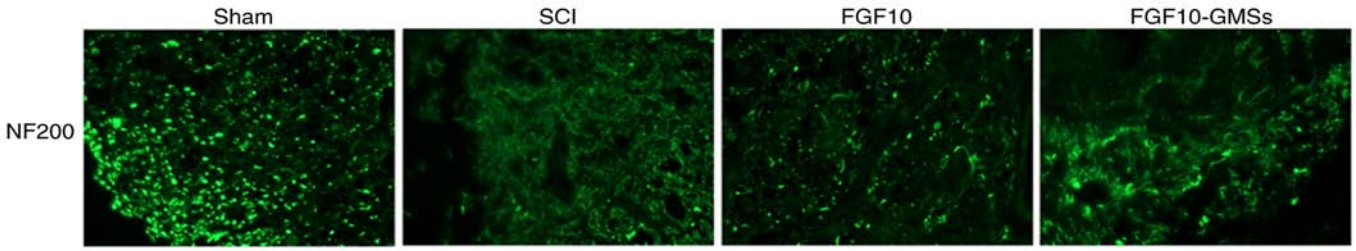

Figure 6. Immunofluorescence staining of NF200 near the site of damage was performed to evaluate the regeneration of injured neurons (magnification, x200; dashed lines denote the injured area). NF200, neurofilament 200; FGF10, fibroblast growth factor 10; GMSs, gelatin microspheres; SCI, spinal cord injury.

inhibitors. FGF10 is highly expressed within the nervous system and is released upon sublethal cellular injury (10,12). However, FGF10 cannot be delivered systemically; as a macromolecular protein, systemic delivery of FGF10 may cause enzyme degradation, and it may also fail to cross the BSCB. Similarly, growth factors are not utilized in the clinical treatment of heart disease due to their low bioactivity and short half-lives with direct *in vivo* injection (27). Furthermore, FGF10 may induce mitosis, which can in turn result in cancer in normal tissues. To resolve these issues, a controlled-release system is needed to improve exogenous growth factor bioavailability.

Previously, implantable porous GMSs have been widely investigated in the context of SCI regeneration due to their tunable physical features and compatibility with molecular and cellular treatments for wounds (20). Notably, implantable bFGF-GMSs facilitate healing in SCI rats and accelerate neurological functional recovery (20). Gelatin hydrogel microspheres appear to be promising as a vehicle for sustained growth factor release in clinical practice, to regenerate injured brain tissues via their action on endogenous neural stem cells (28). In fact, this delivery system is already used extensively in animal models of neurological injury. In the present study, porous GMSs were used for sustained release of FGF10, which was locally implanted into SCI rats to promote neurological functional recovery and neural regeneration. The implantable porous GMSs were based on gelatin and did not show toxicity. Gelatin is biodegradable and biocompatible and thus suitable for implantation into the spinal cord (20). Instead of organic solvents, a w/o emulsion containing materials for fabricating porous microspheres was used. The encapsulated FGF10 easily penetrated the microsphere surfaces of porous GMSs in aqueous solution.

In the rat SCI model of the present study, FGF10-GMS treatment led to superior outcomes in terms of neuroprotection,

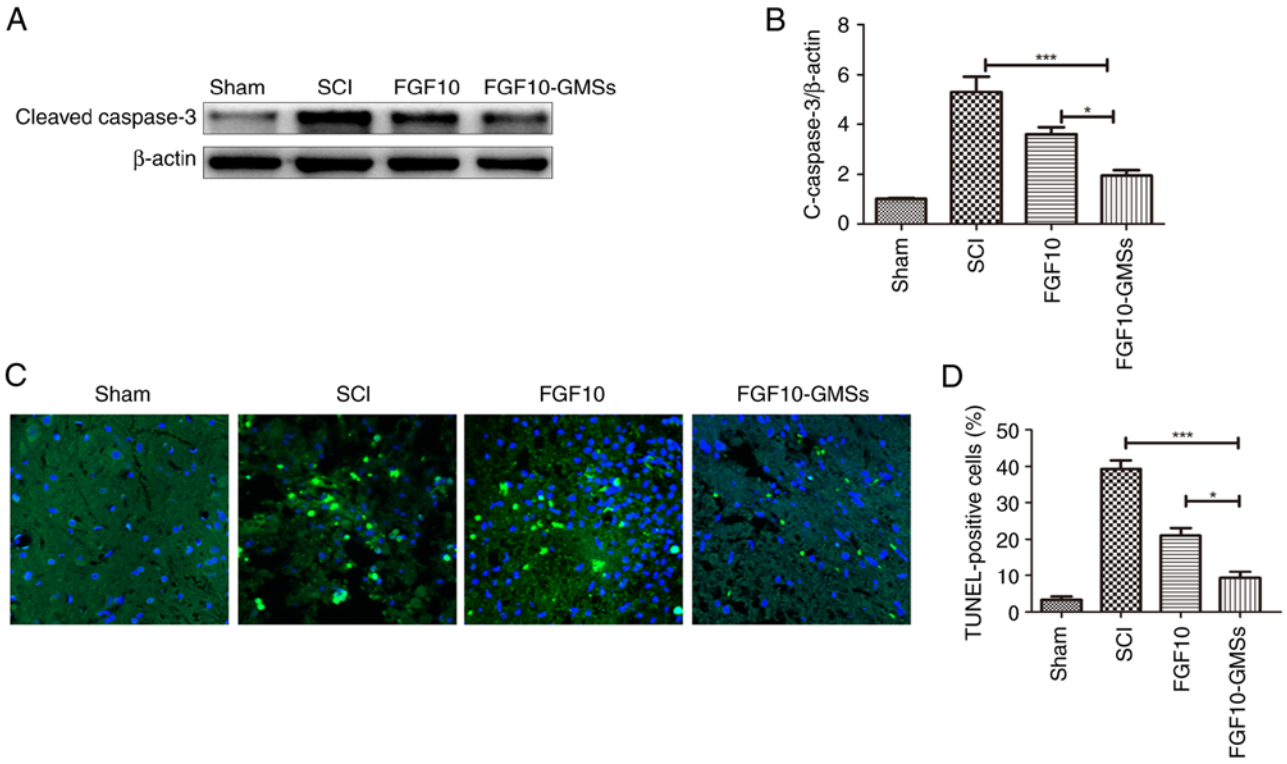

Figure 7. FGF10-GMSs suppress apoptosis in SCI rats compared with free FGF10. (A and B) Expression levels of caspase-3 in each group. (C and D) TUNEL assay was performed to evaluate apoptotic activity in each group. The data are presented as the mean ± SD. *P<0.05 and ***P<0.001. FGF10, fibroblast growth factor 10; GMSs, gelatin microspheres; SCI, spinal cord injury.

motor function and morphological recovery compared with FGF10 treatment. First, FGF10-GMS markedly increased BBB scores and incline plane test performance compared with FGF10. On day 14 after treatment, FGF10-GMS induced more rapid functional recovery in the left hindlimb compared with FGF10 treatment. Second, H&E and Nissl staining showed an obvious protective effect of FGF10-GMS, as reflected by decreased levels of karyopyknosis, necrosis and polymorphonuclear leukocyte infiltration relative to the FGF10 and SCI groups. FGF10 release was significantly extended due to the encapsulation with GMSs, which play an essential role in the critical period for recovery processes, including controlling inflammation and related tissue necrosis. A previous study has revealed the neuroprotective effect of FGF10 on acute brain injury via inhibit inflammation and tissue necrosis (10). Collectively, these data suggested that GMS-loaded FGF10 delivery has huge potential when it was used in the hyperacute period in SCI.

Apoptosis post-SCI modulates neuronal degeneration (29,30). In the present study, FGF10-GMS treatment suppressed apoptosis to a greater degree than did FGF10. The expression of caspase-3, which is an important protein in apoptotic pathways, was decreased following FGF10-GMS treatment, suggesting that caspase-3 exerted anti-apoptotic effects; this was supported by the TUNEL assay results. Immunohistochemical staining of NF200 further verified the neuroprotective effects of FGF10 in SCI rats. It has also been demonstrated that FGF10 enhanced the functional recovery after SCI via inhibition of axonal injury and the FGFR2/PI3K/Akt-dependent apoptosis (12), indicating that GMS-loaded FGF10 delivery has improved neuroprotective effects on axon protection and anti-apoptosis in SCI.

BSCB integrity is important for maintaining spinal cord function. In a previous study, BSCB disruption was detected at 1 h post-injury and persisted for 5 days. Typically, permeability was greatest at 24 h post-injury (31). In the present study, FGF10 reduced EB staining intensity on day 1, which was strongly associated with BSCB penetrability; this effect was even greater in the FGF10-GMS group. Thus, with targeted delivery, FGF10 can cross the BSCB and accumulate at the lesion site more efficiently compared with other administration routes. Furthermore, normal microspheres released FGF10 in rapid bursts; 30% of the encapsulated FGF10 was released within the first 48 h, and 100% was released over the following 2 weeks. By contrast, porous microspheres released FGF10 gradually over 2 weeks, with no burst release pattern observed within the first 48 h. GMS-loaded FGF10 delivery mode can ensure the continuous release of FGF10, reduce the degradation of FGF10 in tissues, and thus continue to play a protective role on injured tissues.

In conclusion, FGF10 has been reported to have anti-inflammatory, anti-apoptotic and axonal protection effects in neurological injury. FGF10 was encapsulated into implantable porous GMSs and released in a sustained manner in SCI rats. This delivery exerted improved neuroprotective effects and created conditions promoting axonal regeneration and functional restoration compared with free FGF10. Therefore, GMS-loaded FGF10 delivery has huge potential when being used in the hyperacute period in SCI.

Acknowledgements

Not applicable.

Funding

The present study was supported by Hainan Natural Science Foundation Youth Fund Project (grant no. 820QN406).

Availability of data and materials

The datasets used and/or analyzed during the current study are available from the corresponding author on reasonable request.

Authors' contributions

YG, TH and YY designed the present study. YG, YY, HQ, HZ and GW contributed to experiments and statistical analysis. YY, HQ and HZ contributed to manuscript preparation and revision for important intellectual content. YG and YY confirm the authenticity of all the raw data. All authors read and approved the final manuscript.

Ethics approval and consent to participate

The present study was approved by the Animal Care and Use Committee of Hainan Medical University (2019-45, Haikou, China).

Patient consent for publication

Not applicable.

Competing interests

The authors declare that they have no competing interests.

References

1. Ren H, Han M, Zhou J, Zheng ZF, Lu P, Wang JJ, Wang JQ, Mao QJ, Gao JQ and Ouyang HW: Repair of spinal cord injury by inhibition of astrocyte growth and inflammatory factor synthesis through local delivery of flavopiridol in PLGA nanoparticles. Biomaterials 35: 6585-6594, 2014.
2. Anjum A, Yazid MD, Fauzi Daud M, Idris J, Ng AMH, Selvi Naicker A, Ismail OHR, Athi Kumar RK and Lokanathan Y: Spinal cord injury: Pathophysiology, multimolecular interactions, and underlying recovery mechanisms. Int J Mol Sci 21: 7533, 2020.
3. Zhang Y, Al Mamun A, Yuan Y, Lu Q, Xiong J, Yang S, Wu C, Wu Y and Wang J: Acute spinal cord injury: Pathophysiology and pharmacological intervention (Review). Mol Med Rep 23: 417, 2021.
4. Kawabata S, Takano M, Numasawa-Kuroiwa Y, Itakura G, Kobayashi Y, Nishiyama Y, Sugai K, Nishimura S, Iwai H, Isoda M, *et al*: Grafted Human iPS cell-derived oligodendrocyte precursor cells contribute to robust remyelination of demyelinated axons after spinal cord injury. Stem Cell Reports 6: 1-8, 2016.
5. Zhang HY, Wang ZG, Wu FZ, Kong XX, Yang J, Lin BB, Zhu SP, Lin L, Gan CS, Fu XB, *et al*: Regulation of autophagy and ubiquitinated protein accumulation by bFGF promotes functional recovery and neural protection in a rat model of spinal cord injury. Mol Neurobiol 48: 452-464, 2013.
6. Assinck P, Duncan GJ, Plemel JR, Lee MJ, Stratton JA, Manesh SB, Liu J, Ramer LM, Kang SH, Bergles DE, *et al*: Myelinogenic plasticity of oligodendrocyte precursor cells following spinal cord contusion injury. J Neurosci 37: 8635-8654, 2017.
7. Kim M, Kim KH, Song SU, Yi TG, Yoon SH, Park SR and Choi BH: Transplantation of human bone marrow-derived clonal mesenchymal stem cells reduces fibrotic scar formation in a rat spinal cord injury model. J Tissue Eng Regen Med 12: e1034-e1045, 2018.
8. Itoh N and Ohta H: Fgf10: A paracrine-signaling molecule in development, disease, and regenerative medicine. Curr Mol Med 14: 504-509, 2014.
9. Chao CM, Moiseenko A, Zimmer KP and Bellusci S: Alveologenesis: Key cellular players and fibroblast growth factor 10 signaling. Mol Cell Pediatr 3: 17, 2016.
10. Li YH, Fu HL, Tian ML, Wang YQ, Chen W, Cai LL, Zhou XH and Yuan HB: Neuron-derived FGF10 ameliorates cerebral ischemia injury via inhibiting NF-κB-dependent neuroinflammation and activating PI3K/Akt survival signaling pathway in mice. Sci Rep 6: 19869, 2016.
11. Dong L, Li R, Li D, Wang B, Lu Y, Li P, Yu F, Jin Y, Ni X, Wu Y, *et al*: FGF10 enhances peripheral nerve regeneration via the preactivation of the PI3K/Akt signaling-mediated antioxidant response. Front Pharmacol 10: 1224, 2019.
12. Chen J, Wang Z, Zheng Z, Chen Y, Khor S, Shi K, He Z, Wang Q, Zhao Y, Zhang H, *et al*: Neuron and microglia/macrophage-derived FGF10 activate neuronal FGFR2/PI3K/Akt signaling and inhibit microglia/macrophages TLR4/NF-κB-dependent neuroinflammation to improve functional recovery after spinal cord injury. Cell Death Dis 8: e3090, 2017.
13. Farooq M, Khan AW, Kim MS and Choi S: The role of fibroblast growth factor (FGF) signaling in tissue repair and regeneration. Cells 10: 3242, 2021.
14. Turner N and Grose R: Fibroblast growth factor signalling: From development to cancer. Nat Rev Cancer 10: 116-129, 2010.
15. Chen L, Zhang Y, Yin L, Cai B, Huang P, Li X and Liang G: Fibroblast growth factor receptor fusions in cancer: Opportunities and challenges. J Exp Clin Cancer Res 40: 345, 2021.
16. Hui Q, Jin Z, Li X, Liu C and Wang X: FGF family: From drug development to clinical application. Int J Mol Sci 19: 1875, 2018.
17. Chang SS, Yokomise H, Matsuura N, Gotoh M and Tabata Y: Novel therapeutic approach for pulmonary emphysema using gelatin microspheres releasing basic fibroblast growth factor in a canine model. Surg Today 44: 1536-1541, 2014.
18. Jin Y, Kim IY, Kim ID, Lee HK, Park JY, Han PL, Kim KK, Choi H and Lee JK: Biodegradable gelatin microspheres enhance the neuroprotective potency of osteopontin via quick and sustained release in the post-ischemic brain. Acta Biomater 10: 3126-3135, 2014.
19. Kempen DH, Lu L, Heijink A, Hefferan TE, Creemers LB, Maran A, Yaszemski MJ and Dhert WJ: Effect of local sequential VEGF and BMP-2 delivery on ectopic and orthotopic bone regeneration. Biomaterials 30: 2816-2825, 2009.
20. Lan L, Tian FR, ZhuGe DL, ZhuGe QC, Shen BX, Jin BH, Huang JP, Wu MZ, Fan LX, Zhao YZ and Xu HL: Implantable porous gelatin microspheres sustained release of bFGF and improved its neuroprotective effect on rats after spinal cord injury. PLoS One 12: e0173814, 2017.
21. Minardi S, Pandolfi L, Taraballi F, De Rosa E, Yazdi IK, Liu X, Ferrari M and Tasciotti E: PLGA-Mesoporous silicon microspheres for the in vivo controlled temporospatial delivery of proteins. ACS Appl Mater Interfaces 7: 16364-16373, 2015.
22. Wang Q, He Y, Zhao Y, Xie H, Lin Q, He Z, Wang X, Li J, Zhang H, Wang C, *et al*: A thermosensitive heparin-poloxamer hydrogel bridges aFGF to treat spinal cord injury. ACS Appl Mater Interfaces 9: 6725-6745, 2017.
23. Basso DM, Beattie MS and Bresnahan JC: A sensitive and reliable locomotor rating scale for open field testing in rats. J Neurotrauma 12: 1-21, 1995.
24. Zheng B, Ye L, Zhou Y, Zhu S, Wang Q, Shi H, Chen D, Wei X, Wang Z, Li X, *et al*: Epidermal growth factor attenuates blood-spinal cord barrier disruption via PI3K/Akt/Rac1 pathway after acute spinal cord injury. J Cell Mol Med 20: 1062-1075, 2016.
25. Liu WG, Wang ZY and Huang ZS: Bone marrow-derived mesenchymal stem cells expressing the bFGF transgene promote axon regeneration and functional recovery after spinal cord injury in rats. Neurol Res 33: 686-693, 2011.
26. Xin DQ, Hu ZM, Huo HJ, Yang XJ, Han D, Xing WH, Zhao Y and Qiu QH: Schisandrin B attenuates the inflammatory response, oxidative stress and apoptosis induced by traumatic spinal cord injury via inhibition of p53 signaling in adult rats. Mol Med Rep 16: 533-538, 2017.

27. Beenken A and Mohammadi M: The FGF family: Biology, pathophysiology and therapy. Nat Rev Drug Discov 8: 235-253, 2009.
28. Nakaguchi K, Jinnou H, Kaneko N, Sawada M, Hikita T, Saitoh S, Tabata Y and Sawamoto K: Growth factors released from gelatin hydrogel microspheres increase new neurons in the adult mouse brain. Stem Cells Int 2012: 915160, 2012.
29. Rong Y, Liu W, Wang J, Fan J, Luo Y, Li L, Kong F, Chen J, Tang P and Cai W: Neural stem cell-derived small extracellular vesicles attenuate apoptosis and neuroinflammation after traumatic spinal cord injury by activating autophagy. Cell Death Dis 10: 340, 2019.
30. Jia G, Zhang Y, Li W and Dai H: Neuroprotective role of icariin in experimental spinal cord injury via its antioxidant, antineuroinflammatory and antiapoptotic properties. Mol Med Rep 20: 3433-3439, 2019.
31. Lee JY, Kim HS, Choi HY, Oh TH and Yune TY: Fluoxetine inhibits matrix metalloprotease activation and prevents disruption of blood-spinal cord barrier after spinal cord injury. Brain 135: 2375-2389, 2012.